Interictal EEG and ECG for SUDEP Risk Assessment: A Retrospective Multicenter Cohort Study

Zhe Sage Chen^{1,2,*}; Aaron Hsieh³; Guanghao Sun¹; Gregory K. Bergey⁴; Samuel F. Berkovic^{5,6}; Piero Perucca^{5,6,11,12,14}, Wendyl D'Souza⁷; Christopher J. Elder⁸; Pue Farooque⁹; Emily L. Johnson⁴; Sarah Barnard^{11,12,16}, Russell Nightscales¹¹⁻¹⁴; Patrick Kwan¹¹⁻¹⁴; Brian Moseley¹⁰; Terence J. O'Brien¹¹⁻¹⁴; Shobi Sivathamboo¹¹⁻¹⁴; Juliana Laze¹⁵; Daniel Friedman^{15,16}; Orrin Devinsky^{2,15,16,*} and the MS-BioS Study Group §

- Department of Psychiatry, New York University Grossman School of Medicine, New York, New York
- ² Neuroscience Institute, New York University Grossman School of Medicine, New York, New York
- ³ Tandon School of Engineering, New York University, New York, New York
- ⁴ Johns Hopkins University School of Medicine, Baltimore, Maryland
- ⁵ Department of Medicine (Austin Health), The University of Melbourne, Heidelberg, Victoria, Australia
- ⁶ Comprehensive Epilepsy Program, Department of Neurology, Austin Health, Heidelberg, 3084, Victoria, Australia.
- Department of Medicine, St. Vincent's Hospital, The University of Melbourne, Fitzroy, Victoria, Australia
- 8 Columbia University, New York, New York
- ⁹ Yale University School of Medicine, New Haven, Connecticut
- ¹⁰ Clinical Development Neurocrine Biosciences Inc., San Diego, California
- Department of Neuroscience, Central Clinical School, Monash University, Melbourne, 3004, Victoria, Australia
- Department of Neurology, Alfred Health, Melbourne, 3004, Victoria, Australia.
- Department of Medicine (The Royal Melbourne Hospital), The University of Melbourne, 3000, Victoria, Australia.
- Department of Neurology, The Royal Melbourne Hospital, Melbourne, 3000, Victoria, Australia.
- 15 Comprehensive Epilepsy Center, New York University Langone Health, New York, New York
- Department of Neurology, New York University Grossman School of Medicine, New York, New York Other contributors of MS-BioS Study Group are listed in Appendix 1.

Corresponding authors:

Zhe Sage Chen, PhD
Department of Psychiatry
New York University School of Medicine
One Park Avenue, Rm 8-226, New York, NY 10016
Email: zhe.chen@nyulangone.org

Orrin Devinsky MD,
Comprehensive Epilepsy Center,
New York University Langone Medical Center
223 E 34th Street, New York, NY 10021
email: Orrin.Devinsky@nyulangone.org

2 tables and 2 figures, 3 supplemental tables, 7 supplemental figures

ORCID

Zhe Sage Chen https://orcid.org/0000-0002-6483-6056
Daniel Friedman https://orcid.org/0000-0003-1068-1797
Orrin Devinsky https://orcid.org/0000-0003-0044-4632

^{*}Correspondence: zhe.chen@nyulangone.org (ZSC) and Orrin.Devinsky@nyulangone.org (OD)

Abstract

Objective: Sudden unexpected death in epilepsy (SUDEP) is the leading cause of epilepsy-related mortality. Although lots of effort has been made in identifying clinical risk factors for SUDEP in the literature, there are few validated methods to predict individual SUDEP risk. Prolonged post-ictal EEG suppression (PGES) is a potential SUDEP biomarker, but its occurrence is infrequent and requires epilepsy monitoring unit admission. We use machine learning methods to examine SUDEP risk using interictal EEG and ECG recordings from SUDEP cases and matched living epilepsy controls.

Methods. This multicenter, retrospective, cohort study examined interictal EEG and ECG recordings from 30 SUDEP cases and 58 age-matched living epilepsy patient controls. We trained machine learning models with interictal EEG and ECG features to predict the retrospective SUDEP risk for each patient. We assessed ross-validated classification accuracy and AUC (area under receiver operating characteristic curve).

Results: The logistic regression (LR) classifier produced the overall best performance, outperforming the support vector machine (SVM), random forest (RF), and convolutional neural network (CNN). Among the 30 SUDEP patients (14 female; mean age [SD], 31 [8.47] years) and 58 living epilepsy controls (26 female [43%]; mean age [SD] 31 [8.5] years), the LR model achieved a median AUC of 0.77 (interquartile range [IQR], 0.73-0.80) in 5-fold cross-validation using interictal alpha and low gamma power ratio of the EEG and heart rate variability (HRV) features extracted from the ECG. The LR model achieved a mean AUC of 0.79 in leave-one-center-out prediction.

Conclusions: Our results support that machine learning-driven models may quantify SUDEP risk for epilepsy patients, future refinements in our model may help predict individualized SUDEP risk and help clinicians correlate predictive scores with the clinical data. Low-cost and noninvasive interictal biomarkers of SUDEP risk may help clinicians identify high-risk patients and initiate preventive strategies.

Keywords: SUDEP, biomarker, machine learning, EEG, ECG

INTRODUCTION

Sudden unexpected death in epilepsy (SUDEP) is the leading cause of epilepsy-related mortality (>3,000 deaths/year in the US), and the second leading neurological cause of lost patient life-years ¹⁻⁴. SUDEP usually occurs during sleep and death are unwitnessed ^{5,6}. Treatment-resistant patients have the highest SUDEP risk. There are currently no validated biomarkers to predict individual SUDEP risk. Risk reduction strategies include convulsive seizure control and nocturnal monitoring ^{3,7,8}. Generalized tonic-clonic seizure (GTCS) frequency and nocturnal convulsions are leading SUDEP risk factors ⁹⁻¹². Supervision during sleep may reduce SUDEP risk. Prolonged post-ictal EEG suppression (PGES) is a potential SUDEP biomarker ¹³⁻¹⁶ but requires epilepsy monitoring unit admission. The cost and potential risk limit PGES, which is available in <5% of epilepsy patients ⁴. Further, non-seizure SUDEP cases can occur, ¹⁷ supporting, the need for interictal biomarkers of SUDEP risk.

Resting-state functional magnetic resonance imaging (fMRI)^{18,19} may detect activity in brainstem cardiopulmonary centers and their cortical connections. Altered resting-state functional connectivity between cortical-subcortical brain regions is implicated in SUDEP²⁰. Large-scale functional brain networks may alter neuronal dynamics, detectable on interictal EEG. Further, heart rate variability (HRV) is a biomarker of autonomic dysfunction and potentially SUDEP risk ²¹⁻²⁵. We recently demonstrated altered HRV in SUDEP cases compared to matched controls ²³. Combining both EEG and ECG measures may improve the efficacy of prediction models. Critically, interictal EEG and ECG are low cost and widely available.

Machine learning has strong predictive power and promising potentials for applications of medical and neurological disorders ²⁶⁻²⁸, and has been increasingly applied to clinical diagnosis and prognosis. Machine learning methods are used for EEG-based seizure detection ²⁹, but infrequently to predict SUDEP risk ^{30-32,33}. We applied machine learning methods to analyze interictal EEG and ECG recordings to assess individualized SUDEP risk. We aimed to identify biomarkers of SUDEP risk and correlate the classification score with clinical variables. We conducted data-driven SUDEP classification and survival analyses and verified the machine-learning models using a retrospective multicenter data cohort.

MATERIALS AND METHODS

Study population and cohort

This multicenter, retrospective, case-control study identified SUDEP cases among patients admitted to eight tertiary epilepsy monitoring units (EMUs) of the MS-BioS Study Group, including the Royal Melbourne Hospital, Austin Hospital, St. Vincent's Hospital, Melbourne, Australia; NYU Langone Health, NY Presbyterian Hospital/Columbia University, New York; University of Cincinnati, Cincinnati; Yale New Haven Hospital, New Haven; and Johns Hopkins Medical Center, Baltimore). Patients who underwent video EEG monitoring (VEM) with >21-scalp electrodes using the 10-20 System and lead II of a standard 12-lead ECG.

Each center identified patients aged 6 months to 65 years with ≥ 1 electroclinical seizure recorded over a 2-11-year consecutive period. All patients were followed for ≥ 5 years. Epilepsy-related deaths were reviewed with available records, medical examiner/coronial and autopsy findings to determine cause of death. We included definite and probable SUDEP cases based on current criteria 34 .

For each SUDEP case, two living epilepsy controls were matched according to admission age (± 4 years), sex, EMU admission year (± 1 year) from the EMU cohort at each center. Epilepsy controls had documented contact in the medical record within six months of screening or were identified as not deceased from national death records.

Demographic and clinical data

For all cases, demographic and clinical data including epilepsy and seizure classification; seizure frequency; age of onset; antiseizure medications (ASMs), epilepsy surgery or neuromodulation; other medications; and medical history (e.g., cardiovascular and psychiatric disorders) were obtained from medical record review at EMU admission.

Recording selection

EEG sampling rate ranged between 256 and 512 Hz. We identified 10-minute interictal segments from non-rapid-eye-movement (NREM) sleep and 10-minute segment from wakefulness during VEM for each case, typically from the first 24-hours of VEM. For most of the studies, we were limited to review of archived EEG which did not include the complete recording and just snippets that were selected for archiving by the clinician. Sleep segments were chosen at random that preceded at least 1 hour before or after a non-convulsive seizure or 6 hours before or after a convulsive seizure. During wakefulness, EEG was collected when subjects were at free of muscle and movement artefact. These artefact-free segments were chosen by a well-trained epileptologist or a research scientist, but were done without the knowledge of any hypothesis. We excluded the immediate post-ictal period, which was defined as ≥6 hours following tonic-clonic seizures (TCS) and ≥1 hour for all other seizure types. EEG and ECG recordings were converted from the proprietary formats to the ASCII format using Persyst 13 (Prescott, Arizona, United States). Similarly, 10-min interictal segments of stable ECG were selected from both NREM sleep and wakefulness (exactly the same time of EEG recordings) for each subject ²⁵.

Off-line EEG and ECG feature computation

For each EEG group signal, we performed band-pass filtering (1-100 Hz), and then computed the relative power ratio at six frequency bands: delta (1-4 Hz), theta (4-8 Hz), alpha (8-15 Hz), beta (15-30 Hz), low gamma (30-50 Hz), high gamma (50-100 Hz). The spectral power was calculated using fast Fourier transform (FFT) with a multi-taper estimator on the entire 10-min recordings. To account for the measurement variability between subjects or centers, we used the relative power percentage and power ratio to calibrate. For instance, the feature derived from the low gamma band was defined as:

```
relative\_low\_gamma\_power = \frac{low\ gamma\ power\ (30-50\ Hz)}{broad\ band\ power\ (1-100\ Hz)}, \\ low\_gamma\_power\_ratio = \frac{relative\_low\_gamma\_power\ (SLEEP)}{relative\_low\_gamma\_power\ (WAKE)}
```

We used the EEG power ratio for the between-subject EEG power calibration purpose. To reduce the feature dimensionality and avoid overfitting, we clustered scalp EEG electrode channels into nine groups (**Figure 1A** and Supplementary Methods). In total, we had 6×9=54 (frequency×group) power ratio features for an individual subject. To further reduce the number of power ratio features, we ranked these EEG features using a linear support vector machine (SVM) classifier (i.e., polynomial kernel with degree 1). The SVM weights associated with individual features determined their relative importance ³⁵. We further selected the most discriminative features ("alpha_power_ratio" and "low_gamma_power_ratio") among specific channel groups.

To analyze ECG recordings, we computed a set of standardized linear (time and frequency-domain) and nonlinear ECG features (a total of 24 ECG-HRV features per subject, see Supplementary Methods and **Figure S1**), and then optimized features. For the sake of feature calibration, we again computed each HRV feature's sleep/wake ratio so that the actual feature was dimensionless. While using the EEG and ECG feature ratios, we did not impose any statistical independence criterion and resorted on an unbiased feature selection procedure. The flowchart of EEG/ECG data analytics is shown in **Figure S2**.

Machine learning methods

We tested multiple standard machine learning methods, including the logistic regression (LR) classifier, linear support vector machine (SVM), and random forest (RF). In all classification methods, the binary label 0/1 represents the non-SUDEP/SUDEP identity in this retrospective study. To alleviate overfitting, simpler models were preferred because of small sample size.

Feature selection

In offline classification task, we considered frequency-specific power ratio features in sleep and wake EEG; and sleep ECG-HRV features. For combined EEG and ECG features, we conducted two systematic approaches to select features. We trained all features with an LR, SVM and RF classifiers with an L_1 norm sparsity constraint, and identified relevant features associated with nonzero regression coefficients after 1000 runs. Next, we retrained the classifier with fewer features without the L_1 norm.

To assess online SUDEP risk, we adopted a sliding window to extract features of the EEG during sleep and then applied the standard machine learning classifiers to the data from each moving window. We employed a parametric CNN architecture (**Figure S3**) with one-dimensional convolutional filters to model the power, frequency and phase relationships between EEG channels ³⁶.

It is noted that we did not include any clinical measurement as the predictive features for two reasons. First, we would like to provide an unbiased analysis without using the clinical diagnostics; instead, we only correlated the predicted risk probability with the clinical variables in the post-hoc analysis. Second, missing data of clinical variables were present in many subjects in this study.

Survival analysis

The clinical variable EMU-to-SUDEP interval (ranged between 0.5 to 10 years) defined the time from EMU recording to the SUDEP incident. To characterize the EMU-to-SUDEP risk in the SUDEP group, we used Cox proportional hazards model with an imposed an L_1 norm sparsity constraint: $\lambda(t|X_i) = \lambda_0 \exp{(X_i\beta)}$, where λ_0 is baseline hazard, X_i are covariates for i-th subject, and β is the regression parameter. The survival analysis was aimed to predict the EMU-to-SUDEP interval with both EEG and ECG features. We used the LASSO method to select the candidate EEG and ECG features 37 . Because of missing data in some SUDEP patients, no other clinical variable was used in the survival analysis. The sparsity constraint on β improved the survival model generalization. The regularization parameter α was estimated by a grid search followed by 5-fold cross validation. We used the concordance index (range 0-1) as the goodness-of-fit assessment, where 1 implies the perfect prediction.

Performance evaluation

The sensitivity, specificity, accuracy and AUC (area under the receiver operating characteristic curve) were calculated for all machine learning classifiers. Median AUC and IQR (25% and 75% percentiles) were computed using 5-fold cross validation with 1000 random repeats. In leave-one-center-out prediction, we used the data from 7 centers to train the model and one center to test the model.

Statistical analysis

Data were analyzed with custom software written in MATLAB and Python. Statistical significance of parametric or nonparametric tests used in all analyses was set at *P*<0.05. Multiple comparisons were corrected using Bonferroni correction. To promote rigor and reproducibility, the data analytic software is shared online (https://github.com/aaronh314/SUDEP).

RESULTS

Study population

Table 1 presents demographic data on the study population (for individual center data, see **Table S1**)²⁵. Data for cases and controls were collected at EMU admission, except for surgical intervention(s) and Engel outcome, collected at last follow-up. The interval between VEEG and SUDEP was 0.5 to 10 years.

We analyzed EEG recordings from 30 SUDEP patients and 58 living epilepsy controls. A subset of 83 subjects had 10-min interictal sleep EEG recordings (In one SUDEP case and four controls, interictal EEG recordings during sleep were unavailable). Furthermore, 76 subjects (26 SUDEP and 50 controls) from this subset had both interictal sleep and wake EEG recordings, and 70 out of these 76 subjects had clean ECG recordings.

TABLE 1. Demographic and clinical characteristics of the study population (modified from Ref. 25)

Characteristic	SUDEP Cases (n=30)	Living Epilepsy Controls (n=58)	<i>P-</i> value
Age – yr, median [IQR]	34 [24, 40]	34 [25, 40]	1.0
Male gender, n (%)	16 (53.3%)	29 (50%)	0.176
Race, n (%)			0.447
White	25 (83.3%)	43 (74.1%)	
Black/African American	3 (10%)	6 (10.3%)	
Asian	1 (3.3%)	3 (5.2%)	
Other	1 (3.3%)	4 (6.9%)	
Unknown	0 (0%)	2 (3.4%)	
Epilepsy classification, n (%)			0.527
Focal	25 (83.3%)	48 (82.8%)	
Generalized	4 (13.3%)	9 (15.5%)	
Combined focal and generalized	1 (3.3%)	1 (1.7%)	
Unknown	0 (0%)	0 (0%)	
Etiology, n (%)			0.583
Structural/Metabolic	15 (50%)	24 (41.4%)	
Genetic/Presumed Genetic	3 (10%)	8 (13.8%)	
Unknown	12 (40%)	26 (44.8%)	
Antiseizure medications on admission, n (%)		0.847
None	0 (0%)	2 (3.4%)	
Monotherapy	4 (13.3%)	11 (19%)	
Polytherapy (≥2)	26 (86.7%)	45 (77.6%)	
Age of onset ‡– yr, median [IQR]	10 [2, 16]	12 [3, 21]	0.571¶
Disease duration – yr, median [IQR]	17 [12, 33]	14 [5, 29]	0.083¶
EMU to SUDEP time – yr, median [IQR]	2 [4, 6]	n/a	n/a
Lifetime tonic-clonic seizure (TCS) frequence	cy§, n (%)		
None	3 (10%)	15 (25.9%)	0.231*
≥1, but <6	3 (10%)	15 (25.9%)	0.231*
≥6, but <50	5 (16.7%)	5 (8.6%)	0.273*
≥50	7 (23.3%)	2 (3.4%)	0.016*
Unknown	12 (40%)	21 (36.2%)	n/a
Outcome of surgical intervention, n (%)			
Engel I	1 (3.3%)	8 (13.8%)	0.264*

Engel II	1 (3.3%)	5 (8.6%)	0.624*	
Engel III	3 (10%)	2 (3.4%)	0.566*	
Engel IV	3 (10%)	1 (1.7%)	0.324*	
Unknown	4 (13.3%)	1 (1.7%)	n/a	
Cardiovascular disease, n (%)				
Hypertension	3 (10%)	4 (6.9%)	0.696	
Cardiac arrhythmia	1 (3.3%)	0 (0%)	0.356	
Structural heart disease	3 (10%)	0 (0%)	0.042	
Sleep apnea	0 (0%)	1 (1.7%)	1.0	
Psychiatric comorbidity, n (%)				
Anxiety disorder	0 (0%)	7 (12.1%)	0.047	
Depression	2 (6.7%)	16 (27.6%)	0.015	
Medication for psychiatric disorder, n (%)				
Antipsychotic	3 (10%)	2 (3.4%)	0.343	

Abbreviation: IQR, interquartile range; EMU, epilepsy monitoring unit.

- ‡ Age of onset unknown in two (3.4%) epilepsy controls.
- \P *P*-value calculated with a two-sample Wilcoxon rank-sum test.
- § Includes both focal-to-bilateral tonic-clonic seizures (TCS) and generalized tonic-clonic seizures (GTCS).
- * Statistical significance corrected p-value following Holm-Bonferroni adjustment for multiple comparisons.

Feature selection, classification and survival analysis

We computed three sets of features: (i) EEG frequency-power ratios during sleep and wake states; (ii) ECG-HRV features, and (iii) sliding window-based sleep EEG features only. For each set, we ranked individual features to compare classification utility. From the combined features (i) and (ii), we identified an optimal subset and compared cross-validated accuracy (**Figure S4**). The optimal set of EEG+ECG features varied between 2 and 5, and we reported the statistics using 3. We trained classifiers using single or combined features separately. For the L_1 regularized LR classifier using features (i)+(ii), the significant coefficients include alpha power ratio, high gamma power ratio, and HRV lf/hf power ratio (**Figure S5**).

In off-line classification, the LR and SVM classifiers achieved comparable or non-significantly different results. The best 5-fold randomized cross-validated AUC (median 0.77, IQR, 0.73-0.80; 1000 Monte Carlo runs) was based on the LR classifier (**Figure 2A** and **Table 2**). Combining EEG and ECG features slightly improved performance for most classifiers, suggesting features are complementary. The low gamma power ratio was significantly higher in the SUDEP patients (especially for EMU-to-SUDEP < 5 years) than controls; most significant in temporal lobes (i.e., EEG groups 4-6; **Figure 1F**). The alpha power ratio was significantly lower in SUDEP cases versus controls (**Figure 1G**). Therefore, low gamma and alpha power ratio from specific regions were most discriminative SUDEP risk features. As a comparison, we also trained ML classifiers using ECG features alone (n=70, based on the same feature selection procedure). After feature ranking, we selected the most discriminative four ECG-HRV features ("Ifnu", "hfnu", "sd1", "ratio_sd2_sd1") for classification analysis, and the cross-validated AUC results were as follows: LR median 0.65 (IQR, 0.61-0.69), SVM median 0.55 (IQR, 0.47-0.62), and RF median 0.58 (IQR, 0.52-0.65).

We performed simulated "on-line" classification based on sleep EEG recordings and found classification accuracy degraded compared to off-line classification. We optimized the window size and features (**Figure S6**), and achieved the best 5-fold cross-validated AUC 0.64 from the LR classifier. The CNN achieved a median AUC 0.60 (IQR, 0.57-0.64), sensitivity 0.45 (IQR, 0.38-0.52), specificity 0.66 (IQR, 0.59-0.73), and accuracy 0.55 (IQR, 0.52-0.57). The simple LR classifier achieved the overall best AUC performance. To test

the model stability in sleep EEG signal non-stationarity, we trained the LR classifier with the first half of sleep EEG and tested the second half; results were comparable, mean cross-validated AUC 0.74 (**Figure S7**).

TABLE 2. Comparison of model performance (median [IQR]) in 5-fold cross-validation

Feature set	# SUDEP + control	Model	AUC	Sensitivity	Specificity	Accuracy
(i)+(ii)	70 = 24 + 46	LR	0.77 [0.73,0.80]	0.63 [0.59,0.67]	0.69 [0.66,0.72]	0.65 [0.62,0.69]
(i)	76 = 26 + 50		0.75 [0.73,0.78]	0.64 [0.60,0.70]	0.68 [0.64,0.72]	0.66 [0.64,0.69]
(iii)	83 = 29 + 54		0.64 [0.60,0.67]	0.73 [0.65,0.79]	0.39 [0.29,0.49]	0.55 [0.50,0.59]
(i)+(ii)	70 = 24 + 46	SVM	0.74 [0.70,0.78]	0.65 [0.57,0.71]	0.64 [0.58,0.71]	0.64 [0.60,0.68]
(i)	76 = 26 + 50		0.74 [0.68,0.78]	0.70 [0.59,0.79]	0.59 [0.53,0.64]	0.63 [0.58,0.68]
(iii)	83 = 29 + 54		0.61 [0.53,0.66]	0.73 [0.59,0.79]	0.40 [0.29,0.49]	0.53 [0.50,0.57]
(i)+(ii)	70 = 24 + 46	RF	0.71 [0.66,0.76]	0.67 [0.62,0.72]	0.66 [0.59,0.71]	0.66 [0.62,0.70]
(i)	76 = 26 + 50		0.61 [0.57,0.66]	0.58 [0.54,0.62]	0.61 [0.54,0.66]	0.59 [0.55,0.63]
(iii)	83 = 29 + 54		0.59 [0.54,0.64]	0.52 [0.45,0.59]	0.63 [0.58,0.69]	0.57 [0.53,0.62]
(iii)	83 = 29 + 54	CNN	0.60 [0.57,0.64]	0.45 [0.38,0.52]	0.66 [0.59,0.73]	0.55 [0.52,0.57]

In the leave-one-center-out prediction setting, only data from seven centers were used to train the model, followed by the validation on the held-out data from the remaining one center. In this case, the LR classifier had mean AUC of 0.734 (min: 0.5, max: 1.0) and mean accuracy of 0.55 (min: 0.25, max: 0.9) (**Table S2**). Thus, the mean AUC result was comparable with the standard 5-fold cross-validation analysis, suggesting moderate generalization at different settings.

In survival analysis within the SUDEP at-risk patients, we obtained the averaged concordance index of 0.687 from 5-fold cross validation (min: 0.44, max: 0.90) from the regularized Cox proportional hazard model with a sparsity constraint. This result was comparable to SUDEP group classification accuracy. The significant coefficients include relative alpha power, the mean heart rate (HR) and the low frequency (LF) power of HRV.

Interpretation of classification results

The AUC statistic can assess diagnostic ability with dichotomous outcomes. Our best off-line AUC performance was 0.74-0.77, acceptable considering the small sample size 38 . Clinically, the sample size is crucial to interpret statistical significance 39,40 . Among the SUDEP patients, the median prediction score showed a negative trend by correlating with the EMU-to-SUDEP time (**Figure 2B**, Pearson's correlation ρ =-0.38, n=26, p=0.054, SVM; ρ =-0.36, p=0.07, LR). SUDEP patients with short-latency (EMU-to-SUDEP time < 5 years) were more accurately classified than those with long-latency (\geq 5 years). Furthermore, SUDEP epilepsy patients with EMU-to-SUDEP time >7 years were misclassified (i.e., treated as false negatives), suggesting that they were closer to living epilepsy controls than other patients with relatively lower SUDEP risk. Epilepsy controls misclassified by LR had low/high gamma power higher in all channels. Additionally, 16.7% of the false positive group, had depression, and 6.7% of the true positive group had depression; 33% of the true negative group had depression. A third of the false positive group had Developmental Delay/Static Encephalopathy, and 40% of the true positive group had Developmental Delay/Static Encephalopathy; 18% of true negatives had Developmental Delay/Static Encephalopathy (**Table S3**).

The CNN can extract informative spatio-spectral features from multichannel EEG data. As the epileptic brain often shows synchronized sleep EEG patterns across brain regions, convolutional filters (2-4 pairs) in the CNN aimed to capture the cross-spectral (amplitude and phase) features between EEG electrodes. To

help visualize these filters, we projected the respective amplitude and phase shift at the same central frequency onto the brain topographies of spatial patterns. The spatial patterns of "amplitude map" indicates the importance at specific channel, whereas the spatial patterns of "phase shift map" indicates the relative phase lagging (**Figure 2C** and Supplementary Methods). At the low frequency (~12.5 Hz), the peak amplitude was grouped around the frontal-temporal lobe electrodes, where the frontal electrodes had a phase lead compared to the central/parietal/occipital electrodes. At the gamma frequency (~33.4 Hz), the peak amplitude was around the temporal lobe, where the occipital electrodes had a phase lag with respect to other electrodes.

DISCUSSION

Our study demonstrates that machine learning tools using interictal EEG and ECG can help distinguish highrisk from low-risk SUDEP patients. Our feature selection procedure identified key interictal EEG or ECG-HRV features in assessing individual SUDEP risk. The CNN extracted complex nonlinear spatiospectral features in sleep EEGs. We plan to refine our model on prospectively ascertained SUDEP and control cohorts. Development of SUDEP biomarker-informed preventive strategies will be the subject of future investigation.

Recently, it has been suggested that ictal biomarkers for PGES/SUDEP based on seizure generation and termination ^{41,42}. It is possible that the ictal episodes may carry the most predictive power for SUDEP risk assessment. However, it remains uncertain if SUDEP risk can be predicted from interictal epileptiform discharges (IEDs) in sleep ^{43,44}. We identified robust differences in EEG sleep/wave power ratio features in low gamma, high gamma and alpha bands between SUDEP and control patients. The effect was pronounced over frontotemporal regions in the scalp EEG recordings, which may correlate with seizure-onset regions; however, detailed investigations are still required to unravel their relationship. An intracranial EEG study has shown that gamma oscillations precede seizure onset zone IEDs ⁴⁵; relative high sleep/wake gamma power ratio may reflect the more frequent IED activity in the SUDEP group. Cross-frequency coupling (e.g., deltagamma phase-amplitude coupling) may improve prediction ⁴⁶. Future studies by integration of multi-stage and multimodal neuroimaging may reveal mechanisms of SUDEP. Furthermore, systematical investigations of the EEG relationship between ictal seizure episodes and interictal episodes will be valuable to understand their contributions to SUDEP. Challenges remain for collection such dataset and development of proper data analytics.

Abnormalities in HRV are linked to sudden cardiac death and SUDEP risk. Patients with drug-resistant epilepsy have more autonomic dysfunction, lower awake HRV and greater variances between wake and sleep states than drug-responsive patients²³. We found reduced LF HRV power was reduced in SUDEP cases and predicted SUDEP latency ²⁵. LF reflects sympathetic and parasympathetic activity. Combining EEG and ECG, improved predictive power over EEG. Analyses combining interictal EEG and new ECG features may improve individual SUDEP prediction ⁴⁷. Large sample size can greatly improve machine learning.

Advancing machine learning models of SUDEP risk will benefit from integration of clinical, imaging and interictal physiological data. Seizure pathways change on circadian and slower timescales ⁴⁸, suggesting that analyzing multiple timescales may provide improve individualized SUDEP prediction, and potentially peak periods of SUDEP risk within circadian or ultradian cycles. Multimodal data fusion techniques can reveal how data modalities interact ⁴⁹ and improve SUDEP prediction ⁵⁰. Greater sample size would greatly improve clinical prognosis and decision ⁵¹⁻⁵³.

Finally, it is also worth pointing out the limitations of our study. Our sample size was relatively small, which may lead to overfitting and limits interpretation. Additionally, the selected EEG and ECG segments were relatively short, and did not cover multiple-day or multiple-session recording samples. We did not assess postictal EEG suppression nor correlate their features with interictal EEG-derived features. Although we have conducted leave-one-center-out validation, the current study did not validate methods on an external patient

population. Finally, our retrospectively acquired cohort prevents validating the classifiers using continuous video-EEG recordings.

CONCLUSION

The results of this analysis suggest that machine learning methods can identify the risk of SUDEP in individual patients in a retrospective multicenter cohort study based on interictal EEG recordings. Combining interictal EEG and ECG-HRV features improves the classification performance. A simple LR classifier produces the overall best classification performance in randomized five-fold cross-validation and leave-one-center-out prediction settings. The CNN can potentially extract multichannel sleep EEG features used for online SUDEP risk assessment. Further studies are warranted to validate the results in larger and more diverse cohorts. The incorporation of other parameters associated with SUDEP (e.g. respiratory measurements and electrodermal activity) may improve the accuracy of models for individual prediction of SUDEP risk.

DATA AVAILABILITY STATEMENT

The data supporting the conclusions of this article will be made by the corresponding authors upon request.

AUTHOR CONTRIBUTIONS

ZSC and OD designed the research. AH and GS analyzed the data. ZSC drafted manuscript, and all authors edited the manuscript. All authors contributed to the article and approved the submitted version.

FUNDING

This study was funded by grants from the US National Institute of Neurological Disorders and Stroke (NINDS, R01-NS123928, R01-NS121776), National Institute of Mental Health (NIMH, R01-MH118928) and National Science Foundation (NSF, CBET-1835000), Multidisciplinary University Research Initiatives (MURI), Centers for Disease Control and Prevention (CDC), Finding a Cure for Epilepsy and Seizures (FACES), and Oracle for Research Award. Aaron Hsieh received a GLASS (Global Leaders and Scholars in STEM) funding from NYU Tandon School of Engineering. The funders had no role in the design and conduct of the study; collection, management, analysis, and interpretation of the data; preparation, review, or approval of the manuscript; and decision to submit the manuscript for publication.

CONFLICT OF INTEREST

Dr. Chen reports grants from the National Institutes of Health (NIH) and National Science Foundation (NSF) during the conduct of the study. Dr. Chen is also a founder and CEO of NeuroThX, LLC. Dr. Chen also received cloud computing resources supported by the Oracle for Research Award. Dr. Friedman receives salary support for consulting and clinical trial related activities performed on behalf of The Epilepsy Study Consortium, a non-profit organization. Dr. Friedman receives no personal income for these activities. NYU receives a fixed amount from the Epilepsy Study Consortium towards Dr. Friedman's salary. Within the past two years, The Epilepsy Study Consortium received payments for research services performed by Dr. Friedman from: Alterity, Baergic, Biogen, BioXcell, Cerevel, Cerebral, Jannsen, Lundbeck, Neurocrine, SK Life Science, and Xenon. He has also served as a paid consultant for Neurelis Pharmaceuticals and Receptor Life Sciences. He has received travel support from the Epilepsy Foundation. He has received research support from NINDS, Epilepsy Foundation, Empatica, Epitel, UCB, Inc and Neuropace unrelated to this study. He serves on the scientific advisory board for Receptor Life Sciences. He holds equity interests in Neuroview Technology. He received royalty income from Oxford University Press. Dr. Berkovic is supported by a Program Grant from the National Health and Medical Research Council of Australia (APP1091593). He reports grants from Eisai, UCB Pharma, and SciGen; has a patent for SCN1A licensed to various diagnostic companies with no financial return, a patent for PRRT2 gene licensed to Athena Diagnostics, and a patent for Diagnostic and Therapeutic Methods for Epilepsy and Mental Retardation Limited to Females (EFMR) licensed to Athena Diagnostics. Dr. Perucca is supported by an Early Career Fellowship from the National Health and Medical Research Council (APP1163708), the Epilepsy Foundation, The University of Melbourne, Monash University, Brain Australia, and the Weary Dunlop Medical Research Foundation. He has received speaker honoraria or consultancy fees to his institution from Chiesi, Eisai, the limbic, LivaNova, Novartis, Sun Pharma, Supernus, and UCB Pharma. He is an Associate Editor for Epilepsia Open. Dr. D'Souza receives salary support from The University of Melbourne. He has received travel, investigator-initiated, scientific advisory board and speaker honoraria from UCB Pharma Australia & Global; investigator-initiated, scientific advisory board, travel and speaker honoraria from Eisai Australia & Global; advisory board honoraria from Liva Nova; educational grants from Novartis Pharmaceuticals, Pfizer Pharmaceuticals and Sanofi-Synthelabo; educational; travel and fellowship grants from GSK Neurology Australia, and honoraria from SciGen Pharmaceuticals. He has shareholdings in the device company EpiMinder. Dr. Kwan is supported by a Medical Research Future Fund from the National Health and Medical Research Council of Australia (MRF1136427) and the Victorian Medical Research Acceleration Fund. He reports grants and personal fees from Eisai, UCB Pharma, and LivaNova; reports grants from Zynerba, Biscayne, and GW Pharmaceuticals; and has received travel, speaker honoraria, or consultancy fees from Sun Pharmaceuticals, Supernus Pharmaceuticals, Novartis, and Eisai. Dr. Moseley is a paid employee at Neurocrine Biosciences Inc. Dr. Moseley has previously served as an advisory board member/consultant for Eisai and UCB Pharma and as a speaker for Eisai, LivaNova and UCB Pharma. He has previously received research support from GW Pharma, LivaNova, Nonin Medical, Inc, Sunovion and Xenon Pharmaceuticals. Dr. O'Brien is supported by a Program Grant (APP1091593) and Investigator Grant (APP1176426) from the National Health and Medical Research Council of Australia and the Victorian Medical Research Acceleration Fund. He reports grants and consulting fees to his institution from Eisai, UCB Pharma, Praxis, Biogen, ES Therapeutics and Zynerba. Dr. Sivathamboo is supported by a Bridging Postdoctoral Fellowship from Monash University (BPF20-3253672466) and the Victorian Medical Research Acceleration Fund. She reports salary support paid to her institution from Kaoskey and Optalert for clinical trial related activities; she receives no personal income for these activities. Dr. Devinsky received grants from the NIH during the conduct of the study, and received funding from Finding A Cure for Epilepsy and Seizures (FACES) and has equity in Empatica. No other disclosures were reported.

REFERENCES

- 1. Thurman DJ, Hesdorffer DC, French JA. Sudden unexpected death in epilepsy: assessing the public health burden. *Epilepsia*. 2014; 55:1479-1485.
- 2. Devinsky O. Sudden, unexpected death in epilepsy. N. Engl. J. Med. 2011; 365: 1801-1811.
- 3. Devinsky O, Hesdorffer DC, Thurman DJ, Lhatoo S, Richerson G. Sudden unexpected death in epilepsy: epidemiology, mechanisms, and prevention. *Lancet Neurol.* 2016; 15:1075-1088.
- 4. Devinsky O, Ryvlin P, Friedman D. Preventing sudden unexpected death in epilepsy. *JAMA Neurology.* 2018; 75:531-532.
- 5. Ali A, Wu S, Issa N, Rose S, et al. Association of sleep with sudden unexpected death in epilepsy. *Epilepsy Behav.* 2017; 76:1-6.
- 6. Mostacci B, Bisulli F, Vignatelli L, et al. Incidence of sudden death in nocturnal frontal lobe epilepsy: a cohort study. *Sleep Med.* 2015; 16: 232-236.
- 7. Surges R, Thijs RD, Tan HL, Sander JW. Sudden unexpected death in epilepsy: risk factors and potential pathomechanisms. *Nat. Rev. Neurol.* 2009; 5: 492.
- 8. Scorza CA, Cavalheiro EA, Scorza FA. SUDEP research: challenges for the future. *Epilepsy Behav.* 2013; 28:134-135.
- 9. Kloster R, Engelskjøn T. Sudden unexpected death in epilepsy (SUDEP): a clinical perspective and a search for risk factors. *J Neurol Neurosurg Psychiatry*. 1999;67:439-444.
- 10. Tomson T, Nashef L, Ryvlin P. Sudden unexpected death in epilepsy: current knowledge and future directions. *Lancet Neurol.* 2008; 7:1021-1031.
- 11. Nashef L, Ryvlin P. Sudden unexpected death in epilepsy (SUDEP): update and reflections. *Neurol Clin.* 2009; 27:1063-1074.
- 12. Ryvlin P, Rheims S, Lhatoo SD. Risks and predictive biomarkers of SUDEP. *Curr. Opin. Neurol.* 2019; 32: 205-212.

- 13. Lhatoo SD, Faulkner HJ, Dembny K, Trippick K, Johnson C, Bird JM. An electroclinical case-control study of sudden unexpected death in epilepsy. *Annals of Neurology*. 2010: 68: 787-796.
- 14. Rajakulendran S, Nashef L. Postictal generalized EEG suppression and SUDEP. *J. Clin. Neurophysiol.* 2015; 32: 14-20.
- 15. Kang JY, Rabiei AH, Myint L, Nei M. Equivocal signficance of post-ictal generalized EEG suppression as a marker of SUDEP risk. *Seizure*. 2017; 48: 28-32.
- 16. Surges R, Strzelczyk A, Scott CA, Walker MC, Sander JW. Postictal generalized electroencephalographic suppressio is associated with generalized seizures. *Epilepsy Behav.* 2011; 21: 271-274.
- 17. Lhatoo SD, Nei M, Raghavan M, et al. Nonseizure SUDEP: sudden unexpected death in epilepsy without preceding epileptic seizures. *Epilepsia*. 2016; 57: 1161-1168.
- 18. Tang Y, Chen Q, Yu X, et al. A resting-state functional connectivity study in patients at high risk for sudden unexpected depth in epilepsy. *Epilepsy & Behavior*, 2014; 41:33-38.
- 19. Allen LA, Harper RM, Lhatoo S, Lemieux L, Diehl B. Neuroimaging of sudden unexpected death in epilepsy (SUDEP): Insights from structural and resting-state functional MRI studies. *Frontiers in Neurology*. 2019;10:185.
- 20. Allen LA, Harper R, Guye M, et al. Altered brain connectivity in sudden unexpected death in epilepsy (SUDEP) revealed using resting-state fMRI. *NeuroImage: Clinical.* 2019; 24: 102060.
- 21. Nei M, Ho RT, Abou-Khalil BW, et al. EEG and ECG in sudden unexplained death in epilepsy. *Epilepsia* 2004; 45(4): 338-345.
- 22. Jeppesen J, Fuglsang-Frederiksen A, Brugada R, et al. Heart rate variability analysis indicates preictal parasympathetic overdrive preceding seizure-induced cariac dysrhythmias leading to sudden unexpected death in a patient with epilepsy. *Epilepsia* 2014; 55: e67-e71.
- 23. Myers KA, Bello-Espinosa L, Symonds JD, et al.. Heart rate variability in epilepsy: a potential biomarker of sudden unexpected death in epilepsy risk. *Epilepsia* 2018; 59: 1372-1380.
- 24. Surges R, Henneberger C, Adjei P, et al. Do alterations in inter-ictal heart rate variability predict sudden unexpected death in epilepsy? *Epilepsy Res.* 2009; 87: 277-280.
- 25. Sivathamboo S, Friedman D, Laze J, et al. Association of short-term heart-rate variability and sudden unexpected death in epilepsy. *Neurology* 2021; 97: e2357-2367.
- 26. Rajkomar A, Dean J, Kohane I. Machine learning in medicine. N Engl J Med 2019; 380:1347-1358.
- 27. Roy Y, Banville H, Albuquerque, et al. Deep learning-based electroencephalography analysis: a systematic review. *J. Neural Eng.* 2019; 16: 051001.
- 28. Gemein LAW, Schirrmeister RT, Chrabaszcz P, et al. Machine-learning-based diagnostics of EEG pathology. *Neuroimage*, 2020; 220: 117021.
- 29. Abbasi B, Goldenhoz DM. Machine learning applications in epilepsy. Epilepsia 2019; 60: 2037-2047.
- 30. Zhu C, Kim Y, Jiang X, Lhatoo S, et al. A lightweight convolutional neural network for assessing an EEG risk marker for sudden unexpected death in epilepsy. *BMC Medical Informatics and Decision Making* 2020; 20: 329.
- 31. Lamichhane B, Kim Y, Segarra S, et al. Automated detection of activity onset after postictal generalized EEG suppression. *BMC Medical Informatics and Decision Making* 2020; 20: 327.
- 32. Mier JC, Kim Y, Jiang X, Zhang GQ, Lhatoo S. Categorisation of EEG suppression using enhanced feature extraction for SUDEP risk assessment. *BMC Medical Informatics and Decision Making* 2020; 20: 326.
- 33. Odom N, Bateman LM. Sudden unexpected depth in epilepsy, peri-ictal physiology and the SUDEP-7 inventory. *Epilepsia*, 2018; 59(10): e157-e160.
- 34. Nashef L, So EL, Ryvlin P, Tomson T. Unifying the definitions of sudden unexpected death in epilepsy. *Epilepsia* 2012; 53: 227-233.
- 35. Chang Y-W, Lin C-J. Feature ranking using linear SVM. *JMLR: Workshop and Conference* Proceedings 3: 53-64.
- 36. Li Y, Murias, Major S, Dawson G, Dzirasa K, Carin L, Carlson DE. Targeting EEG/LFP synchrony with neural nets. *Adv. Neural Info. Proc. Syst (NeuroIPS'17)*, Long Beach, CA.
- 37. Tibshirani, R. The Lasso method for variable selection in the Cox model. Stat. Med. 1997; 16: 385-395.
- 38. Mandrekar JN. Receiver operating characteristic curve in diagnosite test assessment. *J. Thoracic Oncology* 2010; 5: 1315-1316.
- 39. Hajian-Tilaki K. Sample size estimation in diagnostic test studies of biomedical informatics. *J. Biomed. Informatics* 2014; 48: 193-204.
- 40. Bujang MA, Adnan TH. Requirements for minimum sample size for sensitivity and specificity analysis. *J. Clin. Diagn. Res.* 2016; 10: YE01-YE06.
- 41. Jirsa VK, Stacey WC, Quilichini PP, et al. On the nature of seizure dynamics. Brain 2014; 137: 2210-2230.

- 42. Bauer PR, Thijs RD, Lamberts RJ, et al. Dynamics of convulsive seizure termination and post-ictal generalized EEG suppression. *Brain* 2017: 140: 655-668.
- 43. Fisher RS, Scharfman HE, deCurtis M. How can we identify ictal and interictal abnormal activity? In Scharfman HE and Buckmaster PS (eds.) *Issues in Clinical Epileptology: A View from the Bench.* 2014; Springer.
- 44. Staba R, Worrell G. What is the importance of abnormal "background" activity in seizure generation? *Adv. Exp. Med. Biol.* 2014; 813: 43-54.
- 45. Ren L, Kucewicz MT, Cimbalnik J, et al. Gamma oscillations precede interictal epileptiform spikes in the seizure onset zone. *Neurology* 2015; 84: 602-608.
- 46. Griogvsky V, Jacobs D, Breton VL, et al. Delta-gamma phase-amplitude coupling as biomarker of postictal generalized EEG suppression. *Brain Communications*, 2020; 2: fcaa182.
- 47. Chyou JY, Friedman D, Cerrone M, et al. Electrocardiographic features of sudden unexpected death in epilepsy. *Epilepsia.* 2016; 57: e135-139.
- 48. Schroeder GM, Diehl B, Chowdhury FA, Duncan JS, et al. Seizure pathways change on circdaian and slower timescales individual patients with focal epilepsy. *Proc. Natl. Acad. Sci. USA* 2020; 117: 11048-11058.
- 49. van de Vel A, Cuppens K, Bonroy B, et al. Non-EEG seizure-detection systems and potential SUDEP prevention: state of the art. *Seizure*. 2013; 22: 345-355.
- 50. Kanezaki A, Kuga R, Sugano Y, Matsushita Y. Deep learning for multimodal data fusion. *Multimodal Scene Understanding: Algorithms, Applications and Deep Learning*, 2019: 9-39. Academic Press.
- 51. Wen Z, Marie-France M, Hammoud MZ, et al. Fear-induced neuroimaging distinguish anxious and traumatized brains. *Translational Psychiatry*, 2021; 11: 46.
- 52. Geng D, Alkhachroum A, Melo Bicchi M, Cajigas I, Chen SZ. Deep learning for robust detection of interictal epileptiform discharges. *J. Neural Eng.* 2021; 18: 056015.
- 53. Li X, Cui L, Zhang G-Q, Lhatoo SD. Can big data guide prognosis and clinical decisions in epilepsy? *Epilepsia*, 2021; 62:S106-S115.

SUPPORTING INFORMATION

Additional supporting information is online.

FIGURE 1. (**A**) Clustering scalp EEG electrodes (10-20 International System) into nine channel groups (G1-G9). (**B**) Comparison of channel-averaged EEG low gamma sleep/wake power ratios between SUDEP Patients and age-matched living epilepsy controls (SUDEP vs. control 1, ** p=0.0033, paired t-test; SUDEP vs. control 2, * p=0.0251). (**C**) Comparison of subject-averaged EEG low gamma sleep/wake power ratios between SUDEP patients and age-matched living epilepsy controls (****, p<0.0001, paired t-test). (**D**, **E**) Similar to panels B and C, except for the alpha band (panel D: n.s., p=0.258 and p=0.719; panel E: ** p=0.009 and * p=0.039, paired t-test). (**F**) Comparison of EEG low gamma sleep/wake power ratios between SUDEP patients and age-matched controls in nine EEG channel groups (**, p=0.0012, two-way ANOVA test; error bar denotes SEM). (**G**) Similar to panel F, except for the alpha band (**, p=0.048, two-way ANOVA test).

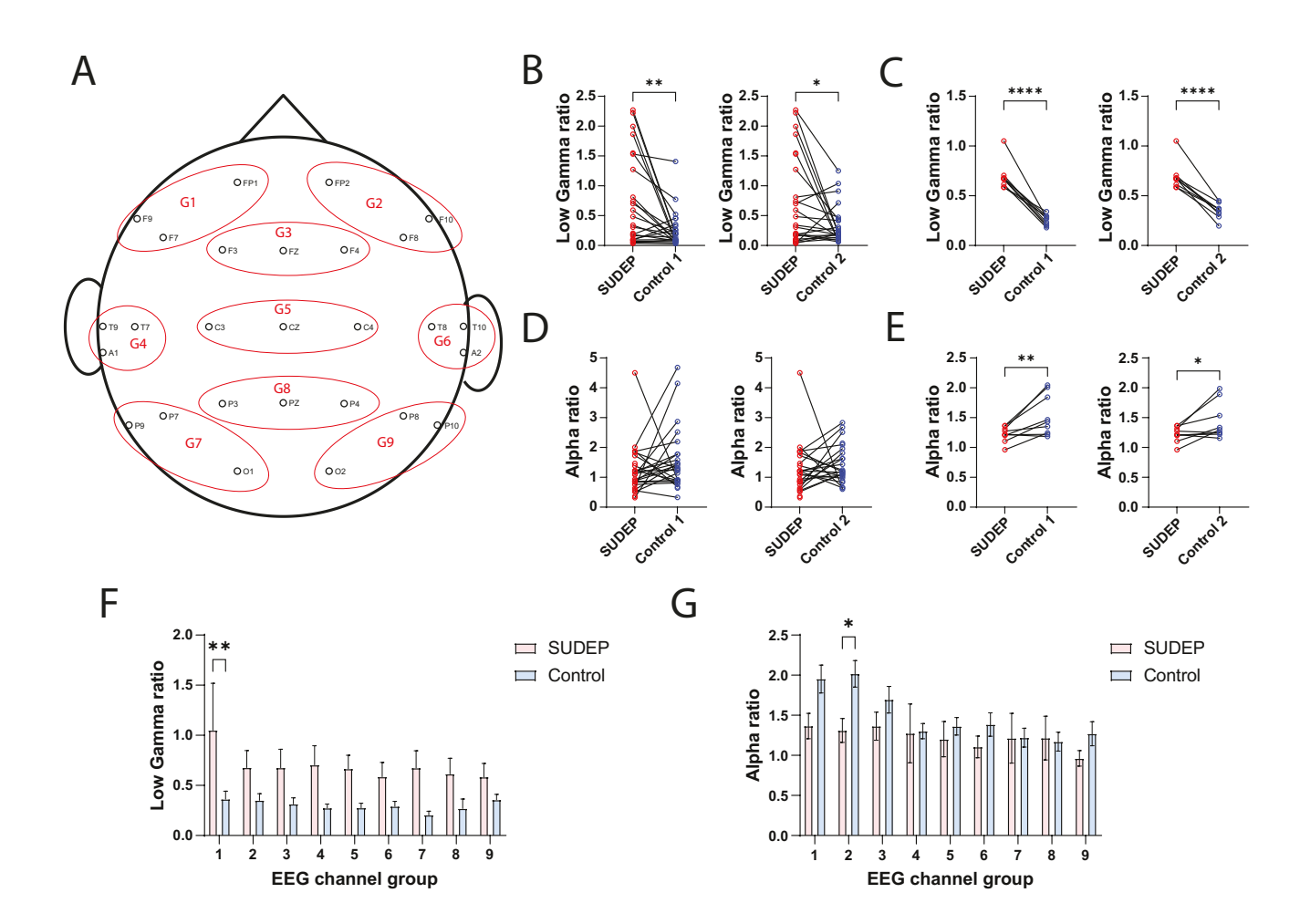
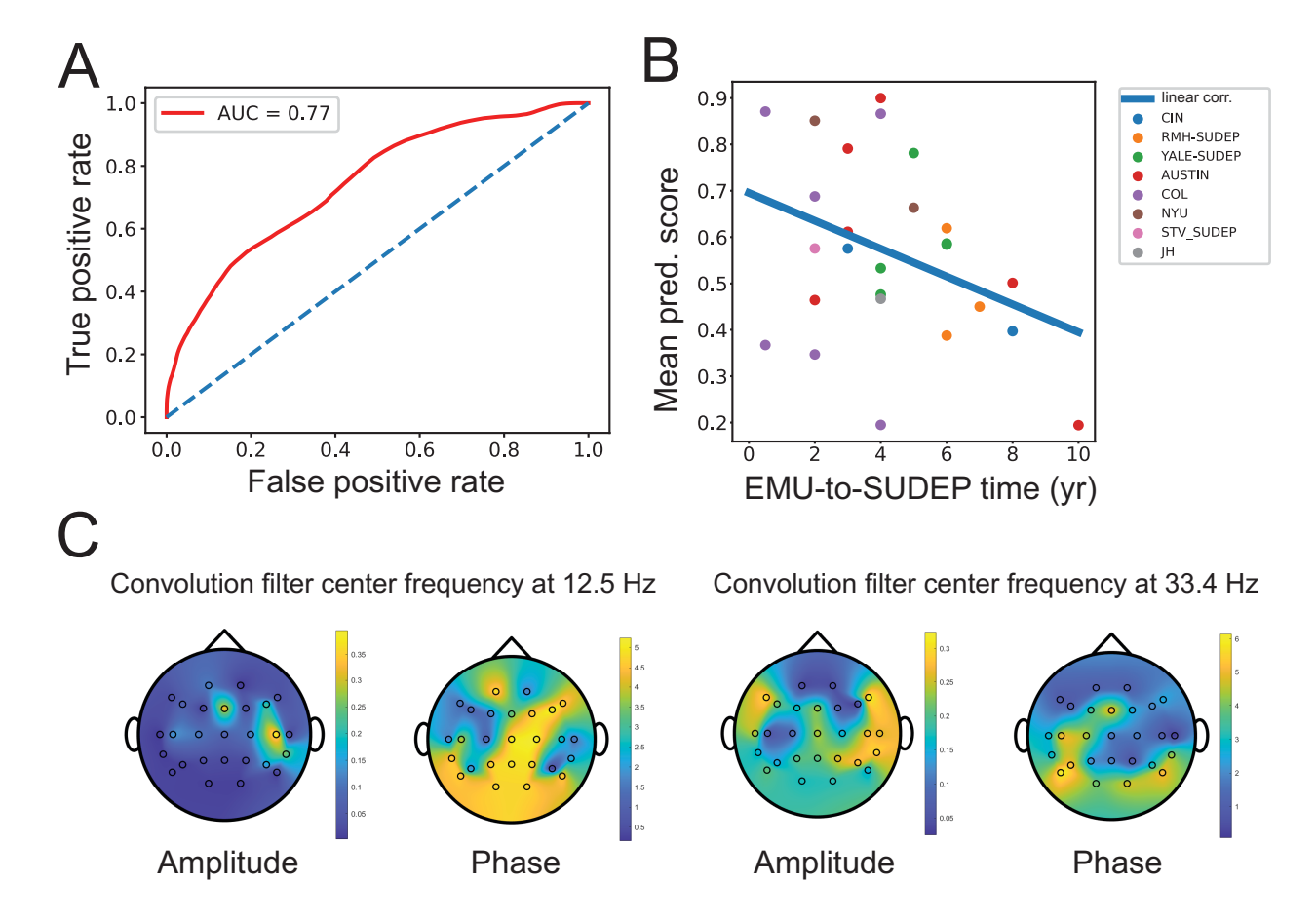


FIGURE 2. (**A**) Mean ROC curve (mean AUC = 0.77, IQR: 0.73-0.80; LR classifier) obtained from SUDEP vs. non-SUDEP classification based on combined EEG and ECG features. Diagonal line shows the chance level (AUC = 0.5). (**B**) The mean SUDEP prediction score correlated negatively with the EMU-to-SUDEP time among the SUDEP group (Pearson's correlation ρ =-0.38, n=26). Color coded points represent patients from 8 different centers. (**C**) Visualization and projection of two pairs of convolutional filters in the CNN onto the brain topographies of spatial patterns. The spatial patterns of "amplitude map" indicates the importance at specific channels, whereas the spatial patterns of "phase shift map" indicates the relative phase lagging.



Supplementary Material

Supplementary Methods

EEG and **ECG** preprocessing and feature selection

Since the EEG data were collected from multiple centers, the recording equipments were not uniform. To accommodate the variability and unify the format of EEG data, we divided EEG channels into 9 groups: G1 ('FP1', 'F7', 'F9'), G2 ('FP2', 'F8', 'F10'), G3 ('FZ', 'F3', 'F4'), G4 ('T7', 'T9', 'A1'), G5 ('T8', 'T10', 'A2'), G6 ('CZ', 'C3', 'C4'), G7 ('P7', 'P9', 'O1'), G8 ('P8', 'P10', 'O2'), G9 ('PZ', 'P3', 'P4'). This division served two purposes. First, the whole brain area was evenly divided into 9 groups on the scalp (**Figure 1A**). Second, regardless of the EEG equipment, and each subject had at least one EEG channel from each channel group. When there were two or three EEG channels within each group, we averaged the data across these channels. Additionally, we further standardized the temporal information. Due to different sampling rates used in various EEG recordings, we resampled all EEG signals with 250 Hz. In total, we computed 6×9=54 (frequency×group) power ratio features per subject.

For ECG signals, we computed a total of 24 linear and nonlinear features for heart rate variabilty (HRV) 1,2:

Time-domain features

Timo domain todiare	
mean_nni	Mean of consecutive R-R intervals
sdnn	Standard deviation of all consecutive normal R-R intervals
sdsd	Standard deviation of differences between R-R intervals
rmssd	Square root of the mean of the sum of the squares of differences
	between adjacent normal R-R intervals
median_nni	Median of absolute values of successive differences of R-R
	intervals
cvsd	RMSSD/mean_nni
cvnni	Coefficient of variation, sdnn/mean_nni
mean_hr	Mean of heart rate
max_hr	Maximum of heart rate
min_hr	Minimum of heart rate
std_hr	Standard deviation of heart rate

Frequency-domain features

vlf	Very low frequency (0-0.04 Hz) parameter
lf	Low frequency (0.04-0.15 Hz) HRV parameter
hf	High frequency (0.15-0.4 Hz) HRV parameter
lf_hf_ratio	LF/HF ratio
lfnu	LF power of HRV expressed in normal units
hfnu	HF power of HRV expressed in normal units
total_power	Total spectral power

Nonlinear-domain features

csi	Cardiac sympathetic index		
cvi	Cardiac vagal index		
Modified csi	Modified CSI		
sd1	Standard deviation along the minor axis of Poincare plot		
Sd2	Standard deviation along the major axis of Poincare plot		
Ratio_sd2_sd1	SD2/SD1 ratio		

Details of CNN training and testing

For the CNN architecture, we used one stream that received *N*-channel raw EEG time series input with *W*-s duration (downsampled at 200 Hz; resulting in a sample size of $200 \times W$). For each stream, we had a set of one-dimensional convolution filters with finite filter length, thereby generating a set of convolution filters (wth size of $m \times N$). Specifically, the *j*-th ($j=1,\dots,m$) convolution filter $f_c^{(j)}$ had a parametric form as a product of cosine function and Gaussian-shape kernel ³

$$f_c^{(j)}(\tau) = A_c^{(j)} \cos\left(\omega^{(j)}\tau + \phi_c^{(j)}\right) \exp\left(-\beta_c^{(j)}\tau^2\right)$$

where the frequency $\omega^{(j)}$ and the precision parameter $\beta_c^{(j)}>0$ were shared across EEG channels (indexed by c), which resembled he real part of a complex Morelet wavelet. In our application, we have tested m=2-4 and used a smallest size m=2 for better interpretability. These two parameters defined the spectral propeties of the filter, where $\omega^{(j)}$ controlled the center of frequency and $\beta_c^{(j)}$ controlled the time-frequency resolution tradeoff. The amplitude $A_c^{(j)}>0$ and phase shift $\phi_c^{(j)}$ were defined for the j-th filter at the c-th channel (or channel group). The output of each convolution filter was a filtered signal acrossed all N channels

$$h^{(j)} = \sum_{c=1}^{N} f_c^{(j)}(t) \otimes x_c(t)$$

The filtered output was passed by a rectified linear unit (ReLU), followed by a max pooling operation. Finally, the feature was flattened, concatenated and sent to the the output layer, which computed a softmax function to produce a prediction score beween 0 (non-SUDEP) and 1 (SUDEP).

To construct the training samples, we specified a window size to create non-overlapping independent "snippets" from each subject's 5-min interictal sleep EEG recording. The cross-entropy loss function was used to assess the CNN training convergence

$$L = \sum_{k=1}^{\text{Batch size}} -[y_k \log \hat{y}_k + (1 - y_k) \log (1 - \hat{y}_k)]$$

Where y_k and \hat{y}_k denote the target and predicted value for the k-th training sample, respectively. We used the batch size of 128.

To train the CNN, we used the Adam algorithm to perform gradient descent optimization ⁴, using a learning rate parameter of 0.1. To avoid overfitting, we also adopted the dropout strategy (probability 0.5) to randomly select the percentage of channels.

During testing, we again used a non-overlapping sliding window and fed multichannel EEG time series into the trained CNN. We computed the prediction scores in the consecutive windows, and then computed an average score by temporal smoothing across multiple sliding windows.

Selection and impact of window duration

The choice of temporal window duration reflected the timescale of interest for the multichannel EEG features. During sleep, EEG oscillations are dominated by slow frequency (<40 Hz). We systematically optimized the window duration to achieve the best performance.

Visualization and interpretation of convolution filters

To visualize the learned spatiospectral features, we mapped the $m \times N$ convolutional filters onto m brain topographies of spatial patterns 3 . Each filter consisted of a spatial pattern of learned amplitude $\{A_c^{(j)}\}$ and phase shift $\{\phi_c^{(j)}\}$, with a specific center frequency $\omega^{(j)}$. For the spatial patterns of "amplitude map", a large value indicates the importance at specific channel or brain region. For the "phase shift map", a value between 0 and π indicates relative phase leading, whereas a value between π and 2π indicates relative phase lagging.

Discussion

The parametric CNN model used in the current paper is motivated from the convolutional neural network (CNN) and deep learning ^{3,5}. Recently, CNNs and recurrent neural networks (RNNs) have been adopted to learn multichannel EEG representations ^{6,7}, in temporal, spectral and spatial domains. Several deep learning models have been proposed in the literature for epilepic EEG signal classification ⁸⁻¹¹, but none of them focused on interictal EEG recordings. As most deep learning models have a large number of model parameters, it is subject to overfitting in the presence of a small training sample size. One effective strategy is to impose a sparsity constraint on the parameterized convolutional filter structure onto the deep learning model ^{3,12}. Additionally, available methods can be applied to assess the importance or sensitivity of features for the outcome of the deep learning models ¹³. With an increasing number of training sample size, the CNN model can potentiall improve the online risk assessment based on interictal EEG during sleep, while offering interpretable neural signatures extracted from the convolutional filters. Finally, explainable Al and explainable deep learning may provide an interface for neurologogists to uncover the state of "epileptic brain".

Supplementary References

- 1. Heart rate variability analysis. https://pypi.org/project/hrv-analysis/. Open source software: https://github.com/Aura-healthcare/hrv-analysis
- 2. Ponnusamy A, Marques JLB, Reuber M. Comparison of heart rate variability parameters during complex partial seizures and psychogenic nonepileptic seizures. *Epilepsia* 2012; 53(8): 1314-1321.
- 3. Li Y, Murias, Major S, Dawson G, Dzirasa K, Carin L, Carlson DE. Targeting EEG/LFP synchrony with neural nets. *Adv. Neural Info. Proc. Syst (NeuroIPS'17)*, Long Beach, CA.
- 4. Kingma DP, Ba J. Adam: A method for stochastic optimization. arXiv preprint. 2014; arXiv:14126980.
- 5. LeCun Y. Bengio Y. Hinton G. Deep learning. Nature 2015: 521: 436-444.
- 6. Bashivan P, Rish I, Yeasin M, Codella N. Learning representations from EEG with deep recurrent-convolutional neural networks. *Proc. Inter. Conf. learned Representations (ICLR'16)*. https://arxiv.org/abs/1511.06448
- 7. Stober S, Sternin A, Owen AM, Grahn JA. Deep feature learning for EEG recordings. *Proc. International Conf. learned Representations (ICLR'16)*. https://arxiv.org/abs/1511.04306
- 8. Zhu C, Kim Y, Jiang X, Lhatoo S, et al. A lightweight convolutional neural network for assessing an EEG risk marker for sudden unexpected death in epilepsy. *BMC Medical Informatics and Decision Making* 2020; 20: 329.
- 9. Gao Y, Gao B, Chen Q, et al. Deep convolutional neural network-based epileptic electroencephalogram (EEG) signal classification. *Front. Neurosci.* 2020; 11: 375.
- 10. Acharya UR, Oh SL, Hagiwara Y, et al. Deep convolutional neural network for the automated detection and diagnosis of seizure using EEG signals. *Computers in Biology and Medicine* 2018; 100: 270-278.
- 11. Lawhern VJ, Solon AJ, Waytowich NR, et al. EEGNet: A compact convolutional network for EEG-based brain-computer interfaces. *J. Neural Eng.* 2018; 15: 056013.
- 12. Mocanu, D.C., Mocanu, E., Stone, P. et al. Scalable training of artificial neural networks with adaptive sparse connectivity inspired by network science. *Nat. Commun.* 2018; 9: 2383.
- 13. Lapuschkin S, Wäldchen S, Binder A, Montavon G, Samek W, Müller K-R. Unmasking Clever Hans predictors and assessing what machines really learn. *Nat. Commun.* 2019;10(1):1096.

TABLE S1: Number of SUDEP and control epilepsy patients from eight centers and leave-one-center-

out performance

Center	# SUDEP	# non-SUDEP	AUC & Accuracy (LR classifier)		
	at-risk	controls	(iii)	(i)	(i)+(ii)
			(n=83)	(n=76)	(n=70)
Melbourne (RMH)	5 (3 F)	8 (4 F)	0.72 [0.68,0.76]	0.56 [0.44, 0.56]	0.50 [0.00, 0.50]
			0.60 [0.50,0.60]	0.50 [0.50,0.67]	0.25 [0.25 0.25]
Melbourne (Austin)	6 (3 F)	12 (6 F)	0.64 [0.61,0.72]	0.78 [0.75, 0.81]	0.96 [0.92, 1.00]
			0.58 [0.50,0.67]	0.75 [0.67,0.75]	0.90 [0.80, 0.90]
Melbourne (St. Vincent)	2 (1 F)	4 (2 F)	0.50 [0.50,0.50]	1.00 [1.00, 1.00]	1.00 [1.00, 1.00]
			0.25 [0.25,0.50]	0.50 [0.50, 1.00]	0.50 [0.50, 0.50]
Columbia University	7 (4 F)	14 (8 F)	0.72 [0.67,0.78]	0.69 [0.64, 0.72]	0.69 [0.64, 0.72]
	, ,	, ,	0.67 [0.58, 0.75]	0.67 [0.58, 0.75]	0.67 [0.67, 0.75]
New York University	2 (0 F)	4 (0 F)	0.75 [0.75,1.00]	0.75 [0.75, 1.00]	1.00 [0.75, 1.00]
			0.75 [0.50, 0.75]	0.75 [0.50, 0.75]	0.75 [0.50, 0.75]
Yale University	5 (2 F)	10 (4 F)	0.36 [0.28,0.44]	0.80 [0.72, 0.84]	0.72 [0.68, 0.76]
-			0.40 [0.30, 0.40]	0.70 [0.60, 0.70]	0.60 [0.50, 0.60]
Johns Hopkins University	1 (0 F)	2 (0 F)	0.75 [0.75,1.00]	1.00 [0.00, 1.00]	0.00 [0.00, 0.00]
,	, ,	, ,	0.50 [0.50, 1.00]	0.50 [0.00, 0.50]	0.00 [0.00, 0.00]
University of Cincinnati	2 (1 F)	4 (2 F)	1.00 [1.00,1.00]	0.75 [0.75, 1.00]	1.00 [1.00, 1.00]
_	, ,	, ,	0.75 [0.50, 0.75]	0.75 [0.50, 0.75]	0.75 [0.75, 0.75]
Total	30 (14 F)	58 (26 F)	Mean: 0.68, 0.56	Mean: 0.79,0.64	Mean: 0.73,0.55

TABLE S2: Comparison of three machine learning classifiers in leave-one-center-out AUC using

features (i)+(ii)

Center	# Total tested subjects (SUDEP+control)	AUC (SVM classifier)	AUC (RF classifier)	AUC (LR classifier)
Melbourne (RMH)	2+5	0.50 [0.25, 0.50]	0.50 [0.25, 0.50]	0.50 [0.00, 0.50]
Melbourne (Austin)	5+12	0.88 [0.80, 0.96]	0.76 [0.66, 0.88]	0.96 [0.92, 1.00]
Melbourne (St. Vincent)	1+1	1.00 [1.00, 1.00]	0.00 [0.00, 0.00]	1.00 [1.00, 1.00]
Columbia University	6+13	0.69 [0.61, 0.72]	0.64 [0.60, 0.71]	0.69 [0.64, 0.75]
New York University	2+4	1.00 [0.75, 1.00]	1.00 [0.75, 1.00]	1.00 [0.75, 1.00]
Yale University	5+8	0.71 [0.64, 0.76]	0.56 [0.46, 0.60]	0.72 [0.68, 0.76]
Johns Hopkins University	1+1	0.00 [0.00, 0.00]	0.00 [0.00, 1.00]	0.00 [0.00, 0.00]
University of Cincinnati	2+2	1.00 [1.00, 1.00]	0.75 [0.75, 0.75]	1.00 [1.00, 1.00]
Total	24+46 = 70	Mean: 0.723	Mean: 0.526	Mean: 0.734

TABLE S3: Statistics of misclassified subjects with depression or developmental delay/static

encephalopathy

	Depression	Developmental Delay/Static Encephalopathy
False Positive	16.7%	33%
True Positive	6.7%	40%
True Negative	33%	18%

Figure S1. Comparison of ECG heart rate variability (HRV) statistics between SUDEP patients and agematched living epilepsy controls. (A) Ifnu. (B) hfnu. (C) If. (D) If/hf ratio. (E) min_hr. (F) std_hr.

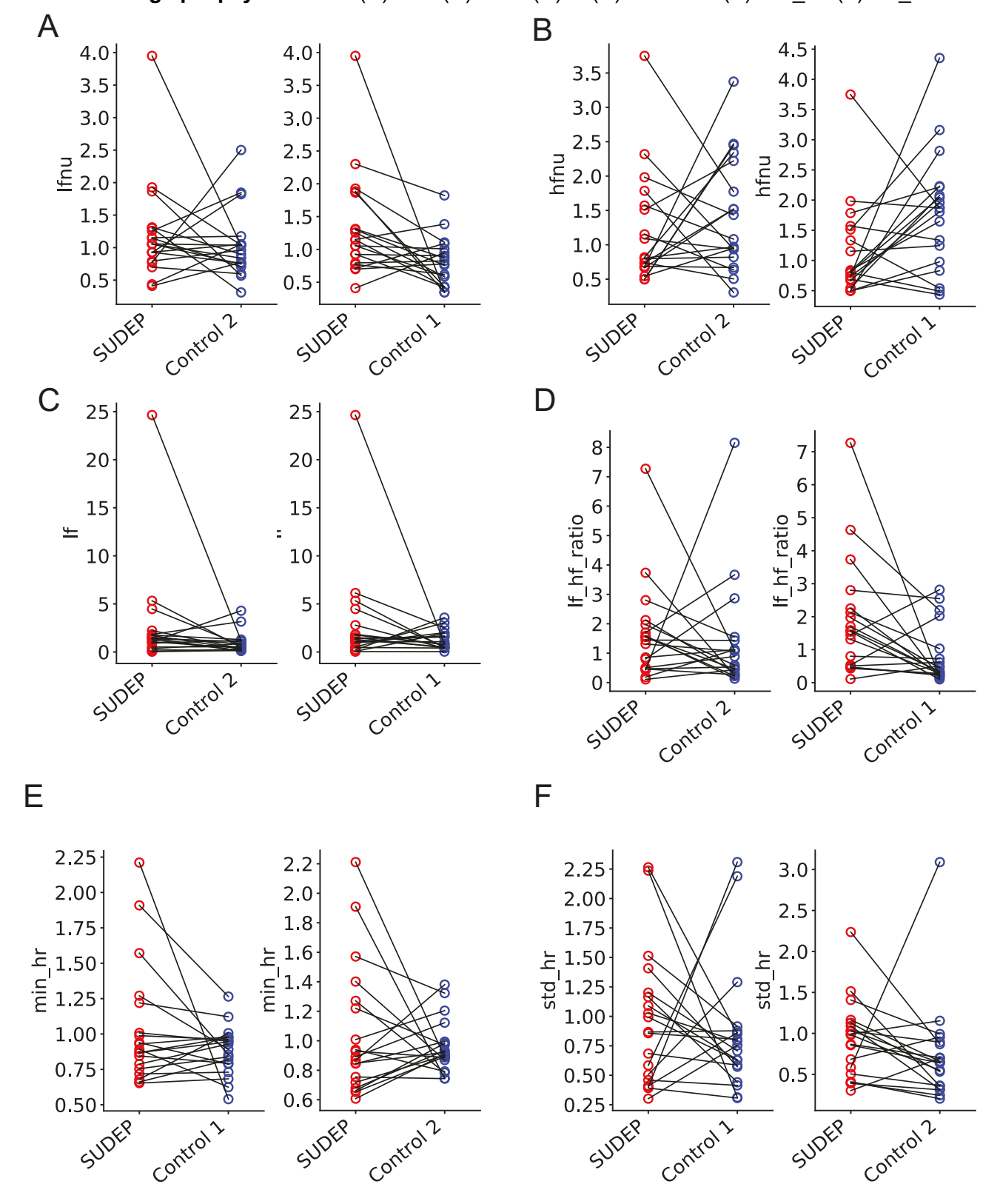


Figure S2. Schematic flowchart of EEG/ECG data analytics in SUDEP risk assessment.

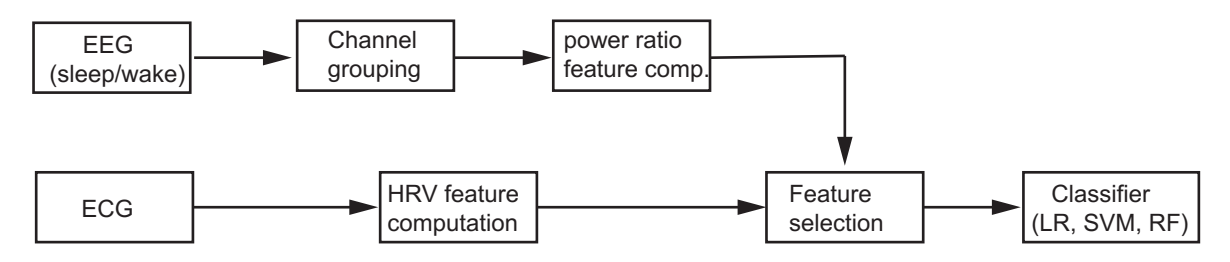


Figure S3. Schematic diagram of convolutional neural network (CNN) for sleep EEG spatiospectral feature extraction, as applied to sliding-window based SUDEP risk assessment. During sleep, multichannel EEG signals were fed to the CNN, which consists of convolution filters, max pooling and flatten operations. These spatiospectral EEG features (mapped onto a brain topography of spatial patterns in heat map) were further sent to a fully connected layer to compute a predictive score between 0 and 1 in the softmax output layer. At the final decision stage, temporal smoothing was applied to the sliding predictive scores to produce a SUDEP risk assessment.

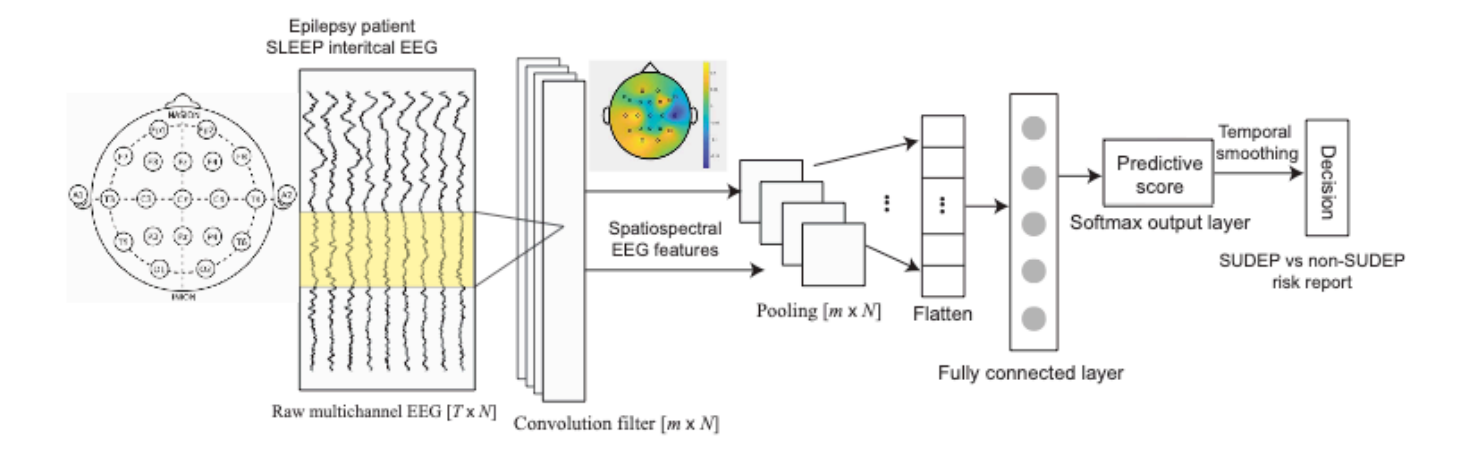


Figure S4. Cross-validated AUC statistics with the number of selected EEG+ECG features. The error bar denotes the SD based on 1000 Monte Carlo runs in the L_1 regularized LR classifier.

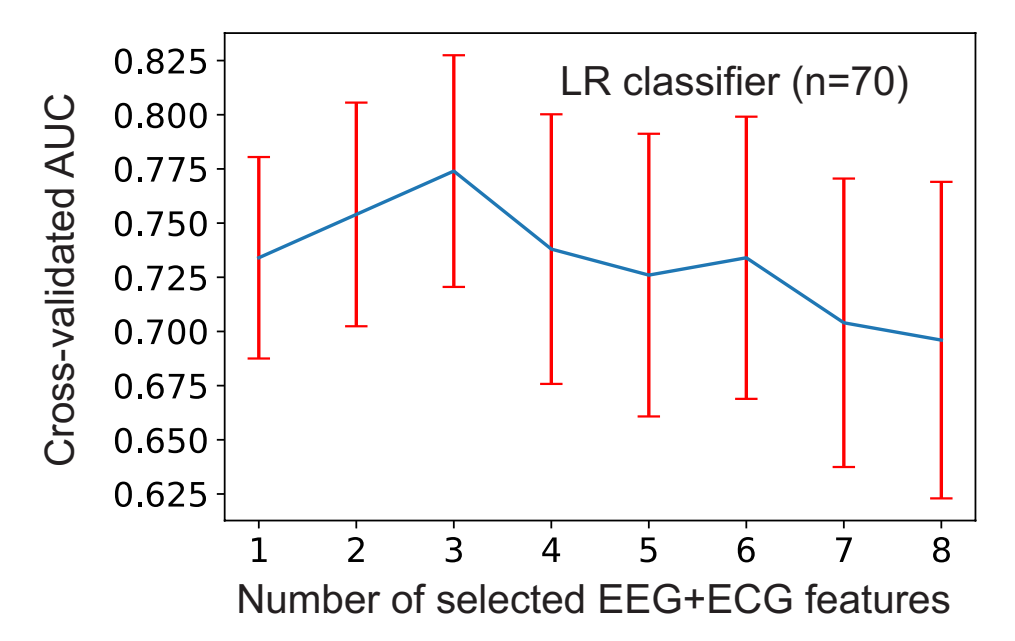


Figure S5. Mean regression coefficients associated with EEG and ECG features used in L_1 regularized LR classifier.

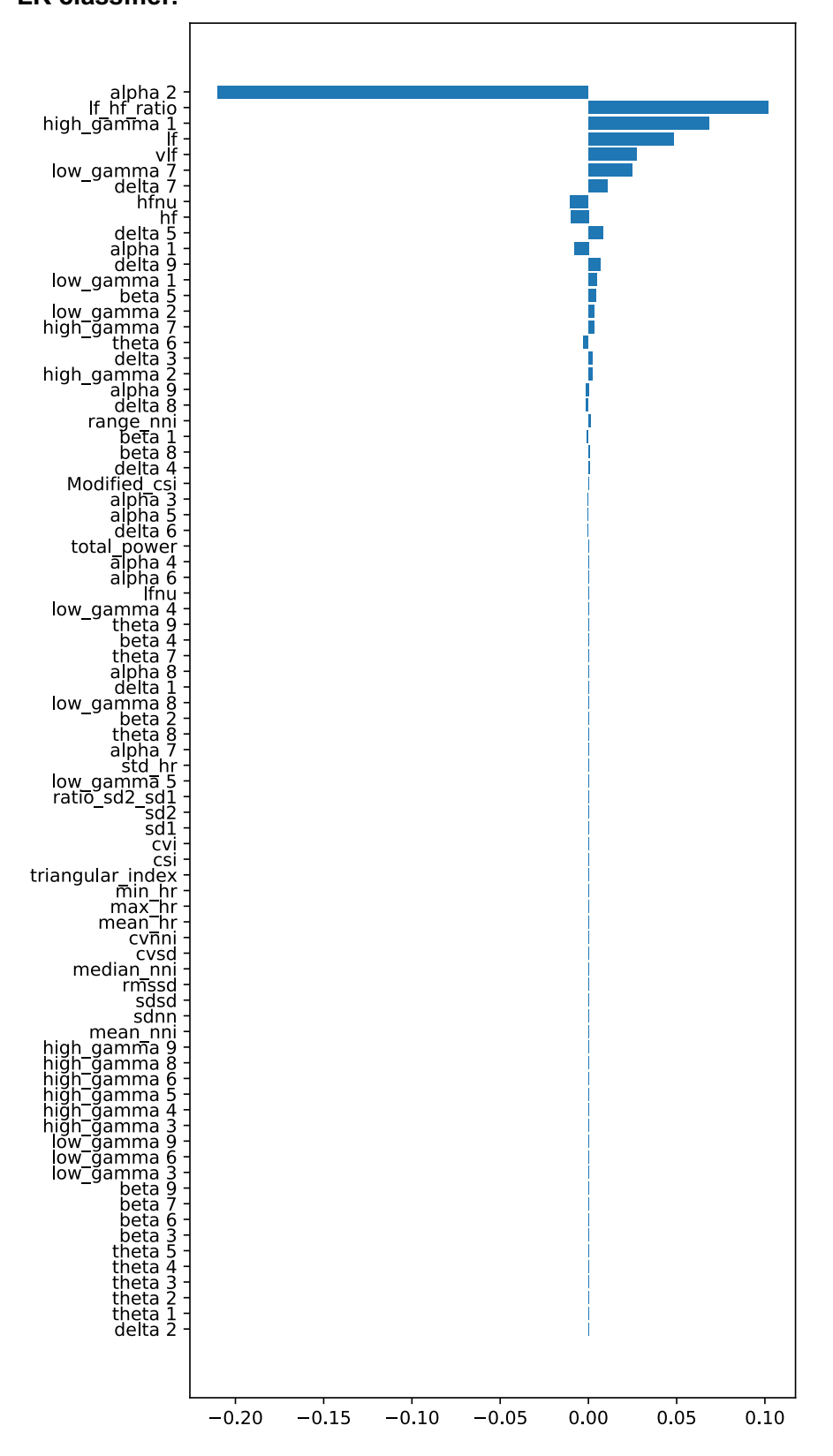


Figure S6. Impact of sliding window duration on online classification performance. In each condition, the box plot statistics were computed based on Monte Carlo runs (n=1000 in LR, and n=100 in CNN).

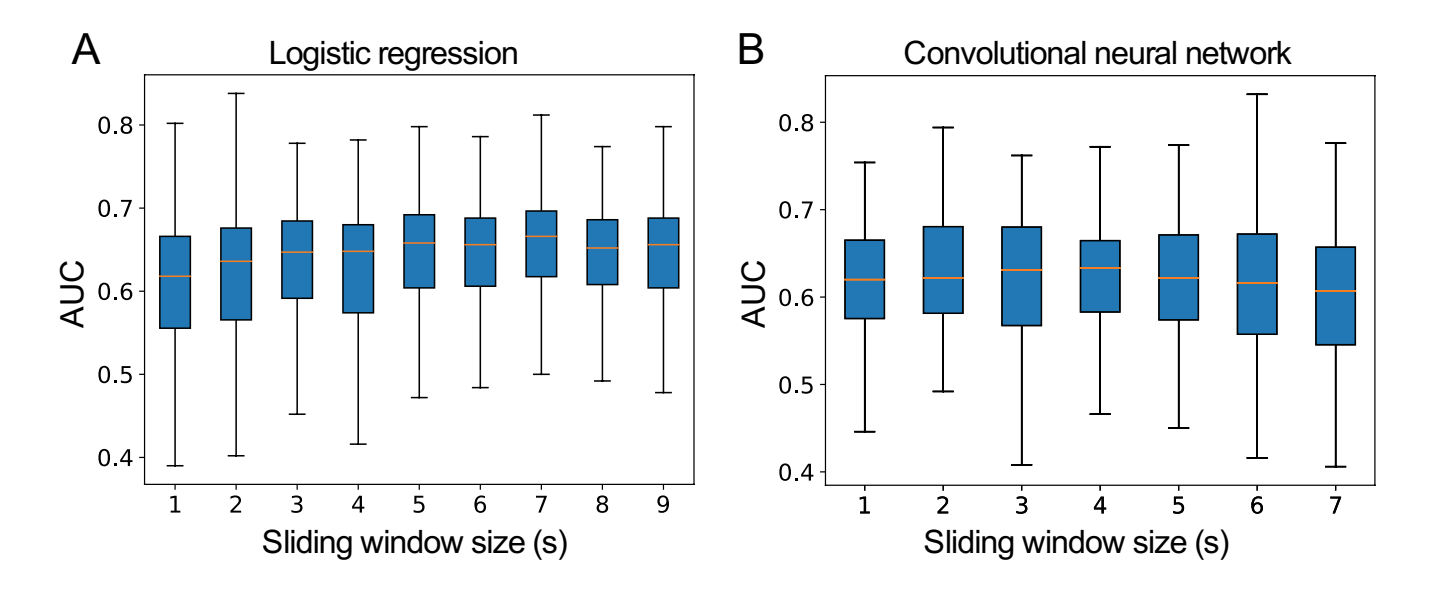
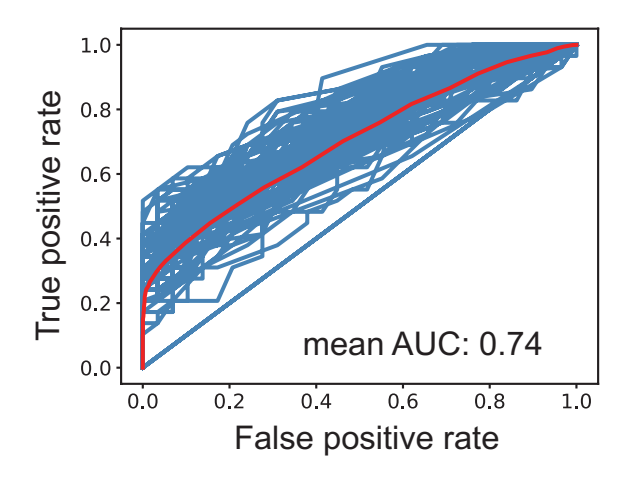


Figure S7. Classification performance was stable in the presence of sleep EEG signal non-stationarity. ROC curves were computed based on training the first half of sleep EEG data and testing the second half of sleep EEG data. Diagonal line indicates the chance level.



Appendix 1: MS-BioS Study Group

Name	Location	Role	Contribution
Dale C. Hesdorffer, PhD	Columbia University,	Principal	Contributed to the acquisition of data.
	New York, United	investigator	
	States		
Sylwia Misiewicz, Ed.M	Columbia University,	Research	Contributed to the acquisition of data.
	New York, United	coordinator	
	States		
Lucy Mendoza, CCRP	University of	Research	Contributed to the acquisition of data.
	Cincinnati, Cincinnati,	coordinator	
	United States		